Heliyon 9 (2023) e18441

Contents lists available at ScienceDirect

Heliyon

journal homepage: www.cell.com/heliyon

Widefield choroidal vasculature associated with future condition of subretinal fluid in central serous chorioretinopathy

Takahiro Kogo, Yuki Muraoka *, Masaharu Ishikura, Naomi Nishigori, Naoko Ueda-Arakawa, Manabu Miyata, Hiroshi Tamura, Masayuki Hata, Ayako Takahashi, Masahiro Miyake, Akitaka Tsujikawa

Department of Ophthalmology and Visual Sciences, Kyoto University Graduate School of Medicine, Kyoto, Japan

ARTICLE INFO

Keywords:
Central serous chorioretinopathy
Widefield swept-source optical coherence tomography
Enhanced depth imaging
Subretinal fluid
Subretinal fluid prognosis
Choroidal thickness
Choroidal vessel diameter index

ABSTRACT

Purpose: To examine choroidal angiographic features in the posterior pole associated with resolution or persistency of subretinal fluid (SRF) in eyes with central serous chorioretinopathy (CSC).
Design: Observational case series.
Methods: Twenty-nine patients with treatment-naïve CSC were divided into two groups based on the presence or absence of SRF 3 months after the initial visit (month 3) without any treatment. Using enhanced depth imaging of widefield swept-source optical coherence tomography, the choroidal thickness (CT), vessel density (VD), and vessel diameter index (VDI) in the superotemporal and inferotemporal subfields on the temporal side of the 18-mm circle from the disc were measured at the initial visit. We calculated the vertical difference in CT and other choroidal angiographic parameters and evaluated their association with the SRF condition at 3 months.
Results: The SRF-resolved and SRF-persistent groups included 10 and 19 patients, respectively. At the initial visit, sex, age, axial length, symptom duration, the logarithm of the minimum angle of resolution visual acuity, and foveal thickness were not significantly different between the two groups. The SRF status at month 3 was not associated with the vertical difference in CT and choroidal VD ($P = .614$, .065, respectively). However, the vertical difference in choroidal VDI was positively associated with the future presence of SRF ($P = .017$).
Conclusions: Vertically asymmetric dilation of choroidal vessels in the posterior pole may be a vasculature feature associated with SRF from CSC and may be a good predictor of future SRF status.

1. Introduction

Central serous chorioretinopathy (CSC) is characterized by subretinal fluid (SRF) in the posterior pole and commonly causes vision impairment in young to middle-aged persons [1,2]. The SRF associated with CSC can spontaneously resolve within several months with no definite symptoms [3,4]. Therefore, SRF is usually managed with observation alone without active treatment. However, in some cases, SRF recurs or persists, and such pathologies can deteriorate the status of the outer segments of photoreceptors and retinal pigment epithelium (RPE), concomitantly impairing visual function [3,5]. Therefore, such cases are indicated for laser photocoagulation or photodynamic therapy (PDT) [3,6,7]. Regarding SRF from CSC, researchers have previously suggested that, in some cases,

* Corresponding author. Department of Ophthalmology, Kyoto University Graduate School of Medicine, Sakyo-ku, Kyoto, 606-8507, Japan.
E-mail address: muraoka@kuhp.kyoto-u.ac.jp (Y. Muraoka).

https://doi.org/10.1016/j.heliyon.2023.e18441
Received 12 January 2023; Received in revised form 27 June 2023; Accepted 18 July 2023
Available online 22 July 2023

optical coherence tomography (OCT) findings of the external limiting membrane slope on SRF can be useful for predicting spontaneous resolution [8]. Specifically, OCT allows non-invasive and detailed evaluations of chorioretinal pathologies [9–11]. Recent technological advances in OCT, especially enhanced depth imaging (EDI), *en face* imaging, and swept-source (SS) OCT, have facilitated the evaluation of the choroidal vasculature and revealed significant pathologies associated with CSC [12–14]. A study using OCT *en face* images showed that the macular choroidal vessels in CSC were more dilated than those in normal eyes [15]. Recent investigations using widefield (WF) SS-OCT have indicated that dilated vortex veins display choroidal thickening from the vicinity of the ampulla to the macula along the course of the veins, suggesting that vortex vein congestion might be involved in the development of CSC [16–18]. However, the choroidal vasculature associated with the CSC-SRF has not been fully elucidated.

In this study, we analyzed the WF SS-OCT data of choroid of eyes with CSC and examined the angiographic feature in the posterior pole that could predict the resolution or prolongation of SRF.

2. Methods

2.1. Patients

This observational study was approved by the Institutional Review Board of the Kyoto University Graduate School of Medicine (Kyoto, Japan) and adhered to the tenets of the Declaration of Helsinki. Written informed consent was obtained from each participant prior to any study procedure or examination.

We included patients with treatment-naïve CSC accompanied by SRF at the macula and presenting with visual symptoms such as visual acuity loss, micropsia, metamorphopsia, and central scotomata within 6 months before the initial examination who visited the Department of Ophthalmology, Kyoto University Hospital between October 2021 and April 2022.

CSC diagnosis was based on the presence of SRF in the posterior pole, which revealed dye leakage from the RPE on fluorescein angiography (FA) and focal choroidal vascular hyperpermeability on late-phase indocyanine green angiography (ICGA). We excluded patients with any of the following: other chorioretinal diseases that could accompany SRF; eyes with macular neovascularization, pit-macular syndrome, uveitis, scleritis, ocular hypertension (>21 mmHg), or hypotension (<5 mmHg); and history of anti-vascular endothelial growth factor treatment (intraocular or extraocular) surgery other than cataract surgery, PDT, direct photocoagulation for the leak point, or administration of corticosteroids. We also excluded patients with keratoconus, high myopia with spherical equivalent < -6 diopters, hyperopia $> +4$ diopters, astigmatism $> \pm 3$ diopters, pregnant women, and eyes with poor-quality OCT images (signal strength index <5) because of eye movement or media opacities. Finally, 29 eyes of 29 consecutive patients met the inclusion criteria and were included in the study. The patients were followed up without any treatment for at least 3 months.

At the initial examination, each patient with CSC underwent extensive ophthalmic assessment with refraction, decimal best-corrected visual acuity testing with a 5-m Landolt chart, intraocular pressure and axial length (AL), slit-lamp biomicroscopy, color fundus photography, FA, ICGA, fundus autofluorescence photography, and SS-OCT. Refraction was objectively measured using an autorefractor, and the spherical equivalent was defined as the sum of the spherical power and half of the cylinder power. We measured the AL using an interferometer (IOL Master 700; Carl Zeiss Meditec, Dublin, CA, USA). Color fundus photography was performed using a fundus camera system (TRC50LX, Topcon Corp., Tokyo, Japan; 3216 × 2136 pixels). FA and ICGA were performed using a confocal scanning laser ophthalmoscope (Spectralis HRA + OCT; Heidelberg Engineering, Heidelberg, Germany).

2.2. Evaluation of macular subretinal fluid

We obtained macular volume scans using spectral domain OCT (Spectralis HRA + OCT, Heidelberg Engineering, Heidelberg, Germany), reviewed all OCT B-scan data for the included patients, and modified the incorrect borders when segmentation errors were generated. Using the Early Treatment Diabetic Retinopathy Study (ETDRS) grid, we created whole-retinal thickness maps centered over the fovea and defined the foveal thickness as the average retinal thickness in the central grid (1 mm in diameter). Retinal thickness calculations were performed using the manufacturer's built-in software (Spectralis Acquisition and Viewing Modules version 6.0; Heidelberg Engineering).

We also evaluated the presence of SRF, and the included eyes were divided into two groups based on the presence or absence of SRF (SRF-resolved group or SRF-persistent group) at 3 months after the initial visit (month 3). We defined the absence of SRF as complete resolution of SRF in the macular OCT B-scan based on the method of the previous report [8]. The judgment was performed by two independent masked retinal specialists (TK and YM).

2.2. Evaluations of choroidal thickness and en face images by EDI of WF SS-OCT

At the initial visit, we examined the choroidal structures using SS-OCT (Xephilio OCT-S1, Canon Medical Systems, Otawara, Japan), with a near-infrared illumination of 1010–1110 nm (scanning laser ophthalmoscope, 780 nm) and a scanning speed of 100,000 A-scans per second. We set the focusing spot of the OCT to 30 mm to ensure that the device could scan a large area. No additional lenses were used or device modifications performed during image acquisition.

To measure the WF changes in the posterior pole, we acquired 3-dimensional volume data of vertical 20 mm (128 B-scans) × horizontal 23 mm (1024 pixels) × scan depth 5.3 mm (1396 pixels) using EDI of SS-OCT. To develop *en face* SS-OCT images, we acquired 3-dimensional volume data of vertical 20 mm (512 pixels) × horizontal 23 mm (512 B-scans) × scan depth 5.3 mm (1396 pixels) in a similar manner. We set the choroidal thickness as the vertical distance from the Bruch's membrane to the chorioscleral

interface to segment the choroid. Segmentation was automatically performed using built-in software supported by artificial intelligence. Most automatic segmentations of the inner and outer borders of the choroid were performed correctly. However, when segmentations were not appropriately performed, we manually corrected the segmentation errors, as required.

2.3. Quantitative measurements on en face images

The vessel density (VD) and vessel diameter index (VDI) were calculated from the choroid en face images based on previous reports' methodology [19,20]. Briefly, after processing with a Gaussian filter [21], the image was binarized with Image*J* software ver. 1.51 (Wayne Rasband, National Institutes of Health, Bethesda, MD, USA; http://rsb.info.nih.gov/ij/index.html). First, the image noise was removed using a Gaussian filter [21]. Then, each image was binarized by the discriminant analysis method [22] using Image*J*'s auto local threshold system. The ratio of the area occupied by the vessels to the total area was calculated as the VD. Next, the binarized images were inverted and skeletonized to measure the total vessel length. Then, the VDI was calculated as the ratio of the total vessel area on the binarized image to the total vessel length on the skeletonized image (Fig. 1). We performed automated image processing and measurement of VD and VDI using Image*J* software.

To evaluate the *en face* images of the choroid, we delineated a circle with an 18-mm diameter and a center coinciding with the center of the fovea. We marked a circle grid surrounding the disc and noise area to avoid evaluating these areas. We divided the 18-mm diameter circle by the vertical line of the disc and horizontal line of the fovea and evaluated the superotemporal and inferotemporal subfields, considering the segmental nature of the choroidal vasculature [23,24]; the venous blood in the choroid drains into its own vortex vein, and the anatomic positions of the ampullae (except for those in patients with high myopia) are usually in the equatorial areas of four quadrants (upper and lower temporal hemispheres and upper and lower nasal hemispheres), whereas the horizontal and vertical watersheds are between the quadrants [18,23,24]. We calculated the VD and VDI at superotemporal (VD_{ST} and VDI_{ST}) and inferotemporal subfields (VD_{IT} and VDI_{IT}). CTs of the same area (CT_{ST} and CT_{IT}) were also evaluated. Considering the vertically asymmetric choroidal vasculature, which was recently considered to be a key pathology of CSC [16–18], we calculated the vertical difference in CT and angiographic parameters of the choroid between the superotemporal and inferotemporal subfields. Moreover, we evaluated their associations with the SRF-resolution at month 3 (Fig. 1).

While measuring the CT and choroidal angiographic parameters, we unified the measurement range among the participants by correcting the AL-related magnification using the modified Littmann formula (Bennett procedure) [25,26].

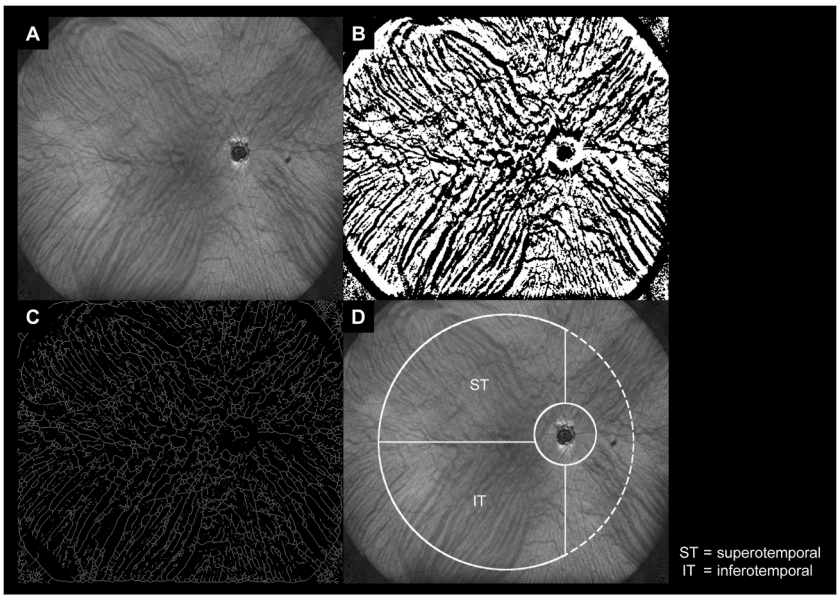

Fig. 1. Quantitative and sectoral evaluations of the choroidal vessels using optical coherence tomography (OCT) for patients with central serous chorioretinopathy. (A) *En face* image of choroid with a scanning area of vertical 20 mm × horizontal 23 mm^2 at the initial visit. (B) Binarized image by the discriminant analysis method after the noise removal by Gaussian filter. (C) Skeletonized image created using the binarized image. The vessel density – the ratio of the area occupied by the vessels to the total area – was assessed on the binarized image. After the skeletonization of the binarized image, the vessel length density – the ratio of the area occupied by the skeleton of vessels to the total area – was calculated. Then, the vessel diameter index, defined as the average vessel caliber, was calculated by dividing the vessel density by the vessel length density. (D) A circle with a diameter of 18 mm, centered on the fovea, was drawn and divided by the vertical line of the disc and the horizontal line of the fovea on the *en face* image. A circle grid was marked surrounding the disc and noise area to avoid evaluating these areas. The choroidal angiographic parameters were calculated in the superotemporal and inferotemporal subfields, and their difference was evaluated. The choroidal thickness in the same area was also calculated.

2.4. Statistical analysis

All data were statistically analyzed using JMP Statistics version 16.0 Pro (SAS Institute Inc., Cary, NC, USA). Values are presented as the mean ± standard deviation. For statistical analysis, BCVA values derived using the Landolt chart were converted to the logarithm of the minimum angle of resolution (logMAR) units.

The Shapiro–Wilk test was used to examine the normal distribution of the data. Levene's test was used to examine the homoscedasticity of the data with a normal distribution. Comparisons between the SRF-resolved and SRF-persistent groups were performed using the Mann-Whitney *U* test for parameters with a non-normal distribution, Welch's *t*-test for parameters with a normal distribution but without homoscedasticity, and unpaired *t*-test for parameters with a normal distribution and homoscedasticity. The chi-squared test was used to evaluate sex differences. Correlations between the visual acuity and other continuous parameters were assessed using the Spearman rank-correlation coefficient. Correlations between other continuous parameters were determined using the Pearson product-moment correlation coefficient after examining the normal distribution of the data. We used JMP Statistics version 16.0 Pro to plot a receiver operating characteristic (ROC) curve and calculated the area under the ROC curve (AUC). In addition, we computed the Youden index to evaluate the sensitivity and specificity of our model. A *P*-value of $< .05$ was considered to indicate statistical significance.

3. Results

In total, we included 29 eyes of 29 patients (22 men and 7 women) with CSC, and all patients had macular SRF at the initial visit (Table 1).

In all cases, the two evaluators agreed upon the judgment of the presence or absence of SRF. Based on the presence or absence of SRF at month 3, 10 patients (34.5%) were categorized into the SRF-resolved group, and 19 patients (65.5%) were categorized into the SRF-persistent group. At the initial visit, sex, age, AL, symptom duration, logMAR BCVA, and foveal thickness were not significantly different between the two groups (Table 2).

At month 3, the mean logMAR BCVAs were 0.00 ± 0.21 for the SRF-resolved group and 0.14 ± 0.19 for the SRF-persistent group; thus, the BCVA of the SRF-persistent group was poorer than that of the SRF-resolved group ($P = .025$, Table 2).

3.1. Comparisons of baseline choroidal parameters between the SRF-resolved- and SRF-persistent groups

Next, we examined the baseline CT and choroidal angiographic parameters of the VD and VDI and compared them between the two groups (Table 3). At the initial visit, the CT, VD, and VDI in the superotemporal and inferotemporal subfields were not significantly different between the two groups (Table 3).

3.2. Baseline vertical differences in choroidal parameters between the SRF-resolved- and SRF-persistent groups

Next, we examined the vertical differences in the parameters between the superotemporal and inferotemporal subfields (Table 3). The vertical differences in the CT and VD did not differ significantly between the groups (Table 3, Figs. 2 and 3).

The vertical differences in the VD and CT were not significantly associated with the logMAR BCVAs at month 3 in either group ($P = .975$, .886 for the SRF-resolved group; $P = .744$ and .884 for the SRF-persistent group, respectively).

3.3. Baseline vertical difference in VDI between the SRF-resolved- and SRF-persistent groups

The vertical difference in VDI was significantly greater in the SRF-persistent group than in the SRF-resolved group ($P = .017$). The vertical difference in VDI was not significantly associated with the logMAR BCVAs at month 3 in either group ($P = .488$ for the SRF-resolved group; $P = .195$ for the SRF-persistent group).

Fig. 4A shows a scatter plot of the vertical difference in VDI. Most eyes with large vertical differences in VDI belonged to the SRF-

Table 1
Characteristics of patients with central serous chorioretinopathy.

Number of patients (women/men)	29 (7/22)
Mean age, years (range, years)	58.3 ± 15.4 (32–85)
Axial length, mm (range, mm)	23.48 ± 0.79 (21.58–24.83)
Initial visit	
Duration of the symptom, months	2.78 ± 1.84
LogMAR visual acuity, (Snellen equivalent)	0.09 ± 0.21 (20/67–20/13)
Foveal thickness, μm	356.1 ± 92.3
Three months after the initial visit	
LogMAR visual acuity, (Snellen equivalent)	0.09 ± 0.21 (20/67–20/13)
Foveal thickness, μm	298.6 ± 53.1

Data are shown as the mean ± standard deviation unless otherwise indicated. LogMAR: logarithm of minimum angle of resolution.

Table 2
Comparisons of clinical characteristics of patients with central serous chorioretinopathy between the subretinal fluid-resolved group and subretinal fluid-persistent group.

	SRF-resolved group	SRF-persistent group	*P*-value
Number of included patients (women/men)	10 (3/7)	19 (4/15)	.593*
Mean age (range), years	53.0 ± 16.2 (32–77)	61.2 ± 14.8 (40–85)	.179**
Axial length, mm	23.63 ± 0.75	23.41 ± 0.83	.508**
Initial visit			
Duration of symptom, months	1.95 ± 1.38	3.21 ± 1.92	.078**
LogMAR visual acuity (Snellen equivalent)	0.03 ± 0.21 (20/67–20/13)	0.13 ± 0.20 (20/67–20/17)	.104**
Foveal thickness, μm	358.2 ± 96.3	354.9 ± 92.7	.982**
Three months after the initial visit			
LogMAR visual acuity (Snellen equivalent)	0.00 ± 0.21 (20/67–20/13)	0.14 ± 0.19 (20/67–20/13)	.025**
Foveal thickness, μm	270.3 ± 42.3	313.4 ± 53.0	.035**

Data are shown as the mean ± standard deviation, unless otherwise indicated.
SRF: subretinal fluid, LogMAR: logarithm of the minimum angle of resolution.
*Comparisons between the SRF-resolved and SRF-persistent groups were performed using chi-squared test for sex differences.
**Comparisons between the SRF-resolved group and SRF-persistent group were performed using unpaired t-test for parameters with normal distribution and homoscedasticity.

Table 3
Comparisons of baseline choroidal parameters of patients with central serous chorioretinopathy between the subretinal fluid-resolved group and subretinal fluid-persistent group.

	SRF-resolved group	SRF-persistent group	*P*-value
Choroidal thickness, μm			
ST	201.3 ± 56.8	198.0 ± 39.3	.855*
IT	166.6 ± 82.2	153.8 ± 45.6	.768**
Vessel density, %			
ST	49.1 ± 3.3	48.1 ± 2.9	.414*
IT	48.2 ± 4.0	46.1 ± 3.1	.123*
Vessel diameter index			
ST	10.05 ± 1.05	10.39 ± 1.06	.415*
IT	9.84 ± 1.04	9.63 ± 0.76	.558*
Difference between choroidal parameters $_{ST}$ and parameters $_{IT}$			
Choroidal thickness, μm	41.5 ± 34.5	48.5 ± 34.1	.614*
Vessel density, %	1.8 ± 1.6	3.2 ± 2.0	.065*
Vessel diameter index	0.66 ± 0.47	1.33 ± 0.95	.017***

Data are shown as the mean ± standard deviation unless otherwise indicated: ST: superotemporal subfield, IT: inferotemporal subfield, SRF: subretinal fluid.
*Comparisons between the SRF-resolved and SRF-persistent groups were performed using the unpaired *t*-test for parameters with normal distribution and homoscedasticity.
**Comparisons between the SRF-resolved group and SRF-persistent group were performed using Mann–Whitney *U* test for parameters without normal distribution.
***Comparisons between the SRF-resolved group and SRF-persistent group were performed using Welch's *t*-test for parameters with normal distribution but without homoscedasticity.

persistent group. We created a ROC curve in which the vertical difference in VDI at the initial visit was set as the independent variable, and the presence or absence of future SRF was set as the dependent variable (Fig. 4B). The AUC was 0.69474. The Youden index showed a vertical difference in VDI of 1.6192; the sensitivity and specificity at this time point were 47.37% and 100.00%, respectively. The vertical difference in the VDI of each group was not associated with the symptom duration before the initial visit ($R = -0.104$, $P = .775$ for the SRF-resolved group; $R = 0.074$, $P = .761$ for the SRF-persistent group). The vertical difference in the VDI of each group was not associated with the symptom duration before the initial visit ($R = -0.039$, $P = .921$ for the SRF-resolved group; $R = 0.211$, $P = .386$ for the SRF-persistent group).

4. Discussion

Using the EDI of SS-OCT, we examined the baseline choroidal vasculature factors associated with the future condition of CSC-SRF without any treatment. Of the baseline choroidal vasculature parameters, the vertical difference in VDI was only significantly associated with the presence of SRF at month 3 (Table 3, Figs. 2–4).

Multiple factors, including genetics, systemic diseases, and corticosteroids, are involved in the development of CSC [6]. Accumulating evidence from WF imaging has shown the characteristic features of the choroid of eyes with CSC, such as vertically and asymmetrically dilated-choroidal veins [27], macular choroidal anastomosis [18], and pulsations [28]. Thus, regarding the pathogenesis of CSC, drainage of the affected vortex veins might be impaired at the scleral outlet, causing choroidal overload (congestion)

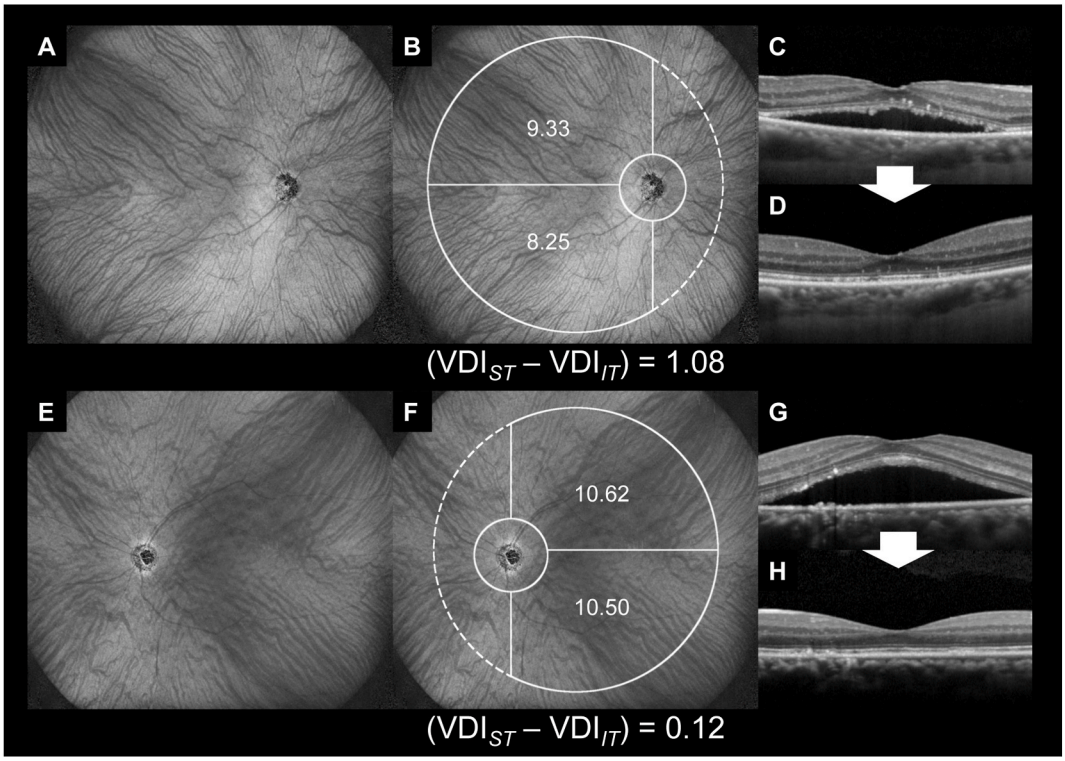

Fig. 2. Representative cases with spontaneously resolved subretinal fluid. (A–D) A 73-year-old man with central serous chorioretinopathy (CSC) in the right eye. At the initial visit, the Snellen visual acuity (VA) was 20/33. Subretinal fluid (SRF) was observed, and the dilation of the choroidal vessel was small (A, B). Three months later, SRF spontaneously resolved, and the Snellen VA improved to 20/25 (C, D).
(E–H) A 43-year-old man with CSC in the left eye. At the initial visit, the VA was 20/17. E and F show that SRF was present, and the choroidal vessels were dilated at both superotemporal and inferotemporal subfields. Three months later, SRF spontaneously resolved, and the Snellen VA was 20/17 (G, H).

and occasionally leading to the development of SRF in the posterior pole [12,29,30].

Sonoda and associates [14,31] evaluated the choroid of eyes with CSC by dividing the whole choroid into superficial and deep layers or stromal and luminal areas using binarized OCT B-scans revealed the structural changes in the choroid of eyes with CSC. However, it is possible that a limited number of OCT B-scans may not adequately evaluate choroidal features in eyes with CSC, as seen extensively in the posterior pole. In this study, we used the EDI of SS-OCT *en face* images to examine the thicknesses and angiographic features of the choroid, partially based on the methodology of previous reports [19,20].

We examined the vertical differences in the WF choroidal structure between the superotemporal and inferotemporal subfields to evaluate the choroidal vasculature of eyes with CSC, which comprise vertically and asymmetrically dilated choroidal veins. In the evaluations, the choroidal structure at the nasal subfields was not examined to omit the effects of image noise on disc locations and the presence of the tips of vertically asymmetric choroidal veins beyond disc-fovea lines.

The condition of the SRF at month 3 was not associated with the vertical difference in CT and VD; instead, it was associated with that of the VDI (Table 3). This means that eyes with large vertical differences in VDI are more likely to have SRF, while eyes with a small vertical difference are more likely to resolve the SRF spontaneously. Some previous studies have indicated that CT is a promising parameter that represents the pathologic conditions of eyes with CSC [13,16,18]. However, CT includes the thicknesses of both choroidal vasculature and stroma [32,33]. Compared to CT, the vertical difference in VDI may better represent the essential feature of the choroid in eyes with CSC (Table 3).

Previous investigations using color fundus photography [34] or fluorescein angiography [35] have shown that SRF development due to diabetic retinopathy (DR) was associated with dilation[41] and increased permeability[42] of the major retinal veins. Previous studies using OCT angiography measured the VD, VLD, and VDI to evaluate retinal vasculature changes. An OCT angiography study showed that the dilated parafoveal capillaries of eyes with retinal vein occlusion were significantly associated with the future recurrence of macular edema [19]. Although the vasculatures are different between the retina and choroid [36], their functional changes in the venous systems can induce SRF [17,37], which is a phenomenon that might be partially common in the retina and choroid.

We speculated that there might be two patterns of choroidal vasculature that facilitate the natural absorption of CSC-SRFs. The first pattern is that the vortex veins are not so dilated on the superotemporal or inferotemporal side, and there is little vertical difference in the VDI. In such cases, the overload (congestion) of the affected vortex veins might be mild, meaning that SRF is unlikely to occur or is

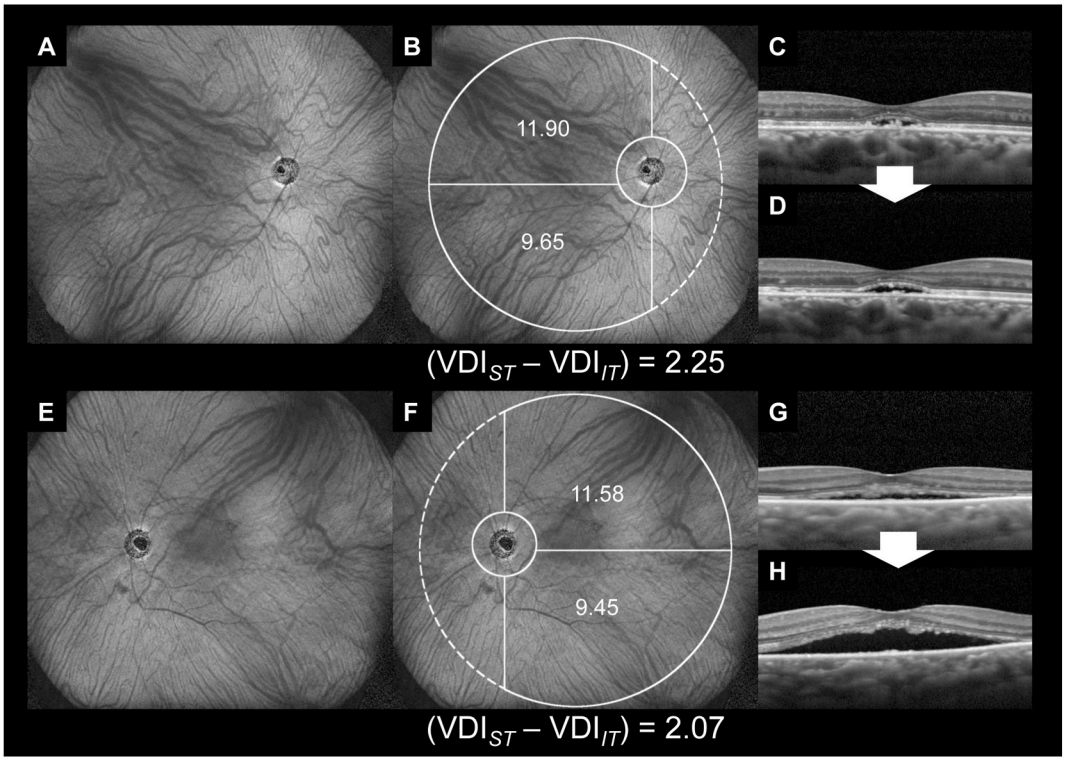

Fig. 3. Representative cases with persistent subretinal fluid. (A–D) A 49-year-old man with central serous chorioretinopathy (CSC) in the right eye. At the initial visit, the Snellen visual acuity (VA) was 20/50. Subretinal fluid (SRF) was observed, and the superotemporal choroidal vessel was dilated (A, B). Three months later, SRF remained, and the Snellen VA was 20/40 (C, D).
(E–H) A 74-year-old woman with CSC in the left eye. At the initial visit, the Snellen visual acuity (VA) was 20/25. SRF was observed, and the superotemporal choroidal vessel was dilated (E, F). Three months later, SRF remained, and the Snellen VA was 20/25 (G, H).

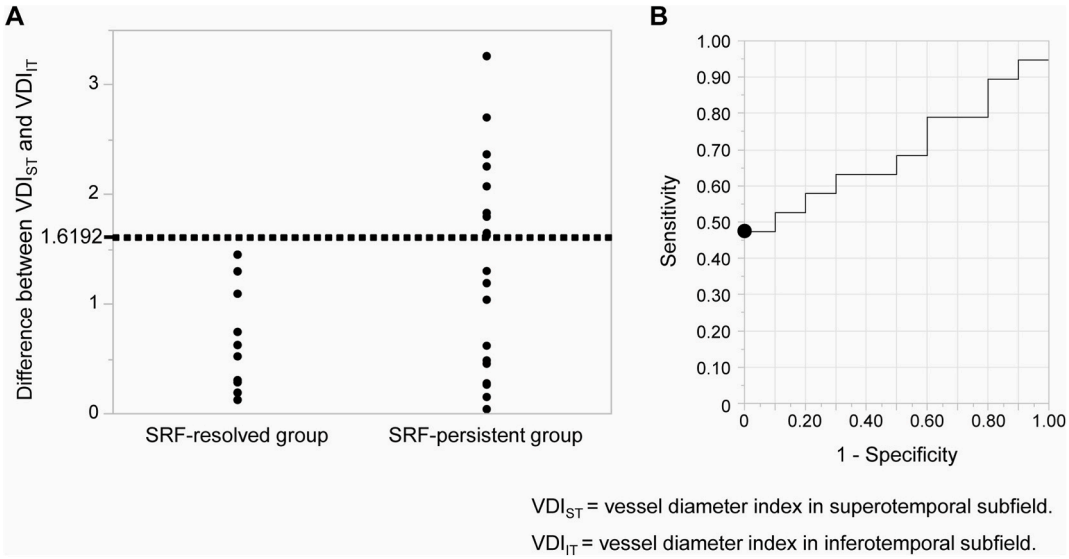

Fig. 4. Scatter plot of the difference in vessel diameter index of each group, receiver operating characteristic (ROC) curve, and cut-off values. (A) Scatter plot of the vessel diameter index (VDI) difference at the initial visit. The difference in the VDI of the SRF-persistent group was significantly larger than that of the SRF-resolved group ($P = .017$). The majority of eyes with large differences in VDI belonged to the SRF-persistent group. (B) The ROC curve is shown for the difference in VDI at the initial visit as the independent variable and whether SRF was persistent or resolved within 3 months from the initial visit as the dependent variable. The area under the curve was 0.69474. The point of the Youden index was at a difference in VDI of 1.6192, at which point, the sensitivity was 47.37%, and the specificity was 100.00%.

likely to resolve in a short period. Another pattern is that the vortex veins are symmetrically dilated on both the superotemporal and inferotemporal sides. Indeed, Matsumoto and associates reported that anastomosis often forms between the superior and inferior vortex veins at the watershed zone in eyes with CSC, allowing the congestive venous blood to bypass the unaffected side [18]. The vertically symmetrically dilated-vortex veins (small vertical difference in VDI) suggest that the anastomosis might function in the resolution of the SRF. In eyes with retinal vein occlusion, macular edema, and SRF occasionally resolve with the formation of collateral vessels at the temporal raphe [38].

In contrast, SRF tends to be persistent in eyes with a large vertical difference in VDI. The asymmetrically dilated choroidal vessels seen in such eyes may indicate that congestive blood flow within the affected vortex vein cannot be sufficiently drained into the opposite (unaffected) side. Evaluating the vertical difference in the VDI in the choroid may be useful for predicting the spontaneous resolution of SRF. Early interventions with PDT may be necessary for eyes with significant vertical differences in VDI to prevent permanent impairment of visual function rather than simply monitoring the condition's progression. By taking this approach, ophthalmologists may be able to prevent irreversible foveal damage and preserve better visual function in patients with CSC.

The present study has some limitations. First, the number of patients included in the study was limited. All patients visited another hospital before the initial visit and were admitted to our hospital according to the hospital's policy. Therefore, patients with CSC whose SRF rapidly resolved might not have been included; thus, the ratio of the SRF-resolved group might be smaller than that in previous reports [3,4]. Second, the duration of symptoms before the initial visit was not unified, and the difference in the duration of symptoms might have affected the results. Third, the duration of this study was only 3 months. In some patients in the SRF-persistent group, the SRF may have resolved after the observation period, which may explain why the SRF-persistent group included eyes with small vertical differences in VDI. Fourth, we evaluated the *en face* images of the whole choroid—the depth of the vortex veins and the more superficial choroidal layer. We did not omit the effect of choroidal vessels other than the vortex veins. Fifth, we did not examine the RPE status around the leak points, which was difficult to accurately and comprehensively identify. Sixth, we divided the evaluation area horizontally by the line of the fovea. However, it was better to objectively and precisely decide the evaluation area by the boundary between the superotemporal and inferotemporal choroidal vessels objectively and precisely. A future study may identify a new way to define the location of the boundary objectively and evaluate the vertical difference more precisely. Finally, we did not evaluate time-dependent changes in *en face* images. Nevertheless, our findings indicate an association between the SRF condition and vertical difference in VDI.

Despite these limitations, the current findings show that the vertical difference in the VDI may be a good predictor of the future conditions of the CSC-SRF without any treatment. Further prospective studies with large cohorts are necessary to confirm our findings and reveal the exact cut-off value of the vertical difference in VDI to predict the status of CSC-SRF.

Declarations

The current observational study was approved by the Institutional Review Board of Kyoto University Graduate School of Medicine (Kyoto, Japan) (approval number: 0352) and adhered to the tenets of the Declaration of Helsinki.

Author contribution statement

Takahiro Kogo; Yuki Muraoka: Conceived and designed the experiments; Performed the experiments; Analyzed and interpreted the data; Contributed reagents, materials, analysis tools or data; Wrote the paper.

Masaharu Ishikura; Naomi Nishigori: Analyzed and interpreted the data; Contributed reagents, materials, analysis tools or data.

Naoko Ueda-Arakawa; Manabu Miyata; Hiroshi Tamura; Masayuki Hata; Ayako Takahashi; Masahiro Miyake; Akitaka Tsujikawa: Contributed reagents, materials, analysis tools or data.

Data availability statement

Data will be made available on request.

Declaration of competing interest

The authors declare the following financial interests/personal relationships which may be considered as potential competing interests: T. Kogo: None, Y. Muraoka: Bayer Yakuhin, Novartis Pharma, Canon, Santen Pharmaceutical, Senju Pharmaceutical, M. Ishikura: None, N. Nishigori: None, N Ueda-Arakawa: Santen Pharmaceutical, Novartis Pharma, Chugai Pharmaceutical, M Miyata: Alcon Japan, Novartis Pharma, Santen Pharmaceutical, HOYA, Bayer Yakuhin, Senju Pharmaceutical, Kowa Pharmaceutical. H Tamura: Findex, Bayer Yakuhin, Novartis Pharma, Santen Pharmaceutical, SUNTORY, Otsuka Pharmaceutical, M Hata: Novartis Pharma, Senju Pharmaceutical, Kyoto Drug Discovery & Development, A. Takahashi: Bayer Yakuhin, Novartis Pharma, Santen Pharmaceutical, MSD, M Miyake: Novartis Pharma, Bayer Yakuhin, Kowa Pharmaceutical, Alcon Japan, AMO Japan, Santen Pharmaceutical, Senju Pharmaceutical, Johnson & Johnson K. K., Chugai Pharmaceutical, A. Tsujikawa: Canon, Findex, Santen Pharmaceutical, Kowa Pharmaceutical, Pfizer, AMO Japan, Senju Pharmaceutical, Wakamoto Pharmaceutical, Alcon Japan, Alcon Pharma, Otsuka Pharmaceutical, Tomey Corporation, Taiho Pharma, HOYA, Bayer Yakuhin, Novartis Pharma, Chugai Pharmaceutical, Astellas, Eisai, Daiichi-Sankyo, Janssen Pharmaceutical, Kyoto Drug Discovery & Development, Allergan Japan, MSD, Ellex, Sanwa Kagaku Kenkyusho, Nitten Pharmaceutical, AbbVie GK.

Acknowledgements

a) Funding/Support: This study was supported in part by a grant-in-aid for scientific research (No. 20K09771) from the Japan Society for the Promotion of Science (Tokyo, Japan), Alcon Japan, Ltd. (Tokyo, Japan), and Canon Inc. (Tokyo, Japan). The funders played no role in the study design, data collection, analysis, decision to publish, or manuscript preparation.

b) Financial Disclosures: None of the authors have proprietary interests in any product described in this article or any conflicts of interest. The authors report the following relationships: T. Kogo: None, Y. Muraoka: Bayer Yakuhin, Novartis Pharma, Canon, Santen Pharmaceutical, Senju Pharmaceutical, M. Ishikura: None, N. Nishigori: None, N Ueda-Arakawa: Santen Pharmaceutical, Novartis Pharma, Chugai Pharmaceutical, M Miyata: Alcon Japan, Novartis Pharma, Santen Pharmaceutical, HOYA, Bayer Yakuhin, Senju Pharmaceutical, Kowa Pharmaceutical. H Tamura: Findex, Bayer Yakuhin, Novartis Pharma, Santen Pharmaceutical, SUNTORY, Otsuka Pharmaceutical, M Hata: Novartis Pharma, Senju Pharmaceutical, Kyoto Drug Discovery & Development, A. Takahashi: Bayer Yakuhin, Novartis Pharma, Santen Pharmaceutical, MSD, M Miyake: Novartis Pharma, Bayer Yakuhin, Kowa Pharmaceutical, Alcon Japan, AMO Japan, Santen Pharmaceutical, Senju Pharmaceutical, Johnson & Johnson K. K., Chugai Pharmaceutical, A. Tsujikawa: Canon, Findex, Santen Pharmaceutical, Kowa Pharmaceutical, Pfizer, AMO Japan, Senju Pharmaceutical, Wakamoto Pharmaceutical, Alcon Japan, Alcon Pharma, Otsuka Pharmaceutical, Tomey Corporation, Taiho Pharma, HOYA, Bayer Yakuhin, Novartis Pharma, Chugai Pharmaceutical, Astellas, Eisai, Daiichi-Sankyo, Janssen Pharmaceutical, Kyoto Drug Discovery & Development, Allergan Japan, MSD, Ellex, Sanwa Kagaku Kenkyusho, Nitten Pharmaceutical, AbbVie GK.

c) Other Acknowledgments: None.

References

[1] M.R. Hee, C.A. Puliafito, C. Wong, et al., Optical coherence tomography of central serous chorioretinopathy, Am. J. Ophthalmol. 120 (1) (1995) 65–74.
[2] A. Kido, M. Miyake, H. Tamura, et al., Incidence of central serous chorioretinopathy (2011-2018): a nationwide population-based cohort study of Japan, Br. J. Ophthalmol. 106 (12) (2022) 1748–1753.
[3] T.J. van Rijssen, E.H.C. van Dijk, S. Yzer, et al., Central serous chorioretinopathy: towards an evidence-based treatment guideline, Prog. Retin. Eye Res. 73 (2019), 100770.
[4] A. Ozkaya, Z. Alkin, M. Ozveren, A.T. Yazici, M. Taskapili, The time of resolution and the rate of recurrence in acute central serous chorioretinopathy following spontaneous resolution and low-fluence photodynamic therapy: a case-control study, Eye (Lond). 30 (7) (2016) 1005–1010.
[5] N.V. Baran, V.P. Gurlu, H. Esgin, Long-term macular function in eyes with central serous chorioretinopathy, Clin. Exp. Ophthalmol. 33 (4) (2005) 369–372.
[6] A. Daruich, A. Matet, A. Dirani, et al., Central serous chorioretinopathy: recent findings and new physiopathology hypothesis, Prog. Retin. Eye Res. 48 (2015) 82–118.
[7] N. Aisu, M. Miyake, Y. Hosoda, et al., Effectiveness of reduced-fluence photodynamic therapy for chronic central serous chorioretinopathy: a propensity score analysis, Ophthalmol Sci 2 (2) (2022), 100152.
[8] H.M.A. Feenstra, J. Hensman, T. Gkika, et al., Spontaneous resolution of chronic central serous chorioretinopathy: “Fuji sign”, Ophthalmol Retina 6 (9) (2022) 861–863.
[9] J.S. Duker, P.K. Kaiser, S. Binder, et al., The international vitreomacular traction study group classification of vitreomacular adhesion, traction, and macular hole, Ophthalmology 120 (12) (2013) 2611–2619.
[10] M. Iglicki, A. Loewenstein, A. Barak, S. Schwartz, D. Zur, Outer retinal hyperreflective deposits (ORYD): a new OCT feature in naive diabetic macular oedema after PPV with ILM peeling, Br. J. Ophthalmol. 104 (5) (2020) 666–671.
[11] D. Zur, M. Iglicki, C. Busch, et al., OCT biomarkers as functional outcome predictors in diabetic macular edema treated with dexamethasone implant, Ophthalmology 125 (2) (2018) 267–275.
[12] N. Terao, N. Imanaga, S. Wakugawa, et al., Ciliochoroidal effusion in central serous chorioretinopathy, Retina 42 (4) (2022) 730–737.
[13] M. Lehmann, B. Wolff, V. Vasseur, et al., Retinal and choroidal changes observed with ‘En face’ enhanced-depth imaging OCT in central serous chorioretinopathy, Br. J. Ophthalmol. 97 (9) (2013) 1181–1186.
[14] S. Sonoda, T. Sakamoto, N. Kuroiwa, et al., Structural changes of inner and outer choroid in central serous chorioretinopathy determined by optical coherence tomography, PLoS One 11 (6) (2016), e0157190.
[15] H. Shiihara, S. Sonoda, H. Terasaki, et al., Quantitative analyses of diameter and running pattern of choroidal vessels in central serous chorioretinopathy by en face images, Sci. Rep. 10 (1) (2020) 9591.
[16] M. Ishikura, Y. Muraoka, N. Nishigori, et al., Widefield choroidal thickness of eyes with central serous chorioretinopathy examined by swept-source OCT, Ophthalmol Retina 6 (10) (2022) 949–956.
[17] S. Kishi, H. Matsumoto, A new insight into pachychoroid diseases: remodeling of choroidal vasculature, Graefes Arch. Clin. Exp. Ophthalmol. (2022) 1–3.
[18] H. Matsumoto, J. Hoshino, R. Mukai, et al., Vortex vein anastomosis at the watershed in pachychoroid spectrum diseases, Ophthalmol Retina 4 (9) (2020) 938–945.
[19] T. Kogo, Y. Muraoka, A. Uji, et al., Angiographic risk factors for recurrence of macular edema associated with branch retinal vein occlusion, Retina 41 (6) (2021) 1219–1226.
[20] A. Uji, S. Balasubramanian, J. Lei, E. Baghdasaryan, M. Al-Sheikh, S.R. Sadda, Impact of multiple en face image averaging on quantitative assessment from optical coherence tomography angiography images, Ophthalmology 124 (7) (2017) 944–952.
[21] J. Mazzaferri, L. Beaton, G. Hounye, D.N. Sayah, S. Costantino, Open-source algorithm for automatic choroid segmentation of OCT volume reconstructions, Sci. Rep. 7 (2017), 42112.
[22] N. Otsu, A threshold selection method from gray-level histograms, Man Cybern 9 (1979) 62–66.
[23] S.S. Hayreh, Segmental nature of the choroidal vasculature, Br. J. Ophthalmol. 59 (11) (1975) 631–648.
[24] S.S. Hayreh, In vivo choroidal circulation and its watershed zones, Eye (Lond). 4 (Pt 2) (1990) 273–289.
[25] A.G. Bennett, A.R. Rudnicka, D.F. Edgar, Improvements on Littmann’s method of determining the size of retinal features by fundus photography, Graefes Arch. Clin. Exp. Ophthalmol. 232 (6) (1994) 361–367.
[26] S. Kadomoto, Y. Muraoka, S. Ooto, et al., Evaluation of macular ischemia in eyes with branch retinal vein occlusion: an optical coherence tomography angiography study, Retina 38 (2) (2018) 272–282.
[27] T. Hiroe, S. Kishi, Dilatation of asymmetric vortex vein in central serous chorioretinopathy, Ophthalmol Retina 2 (2) (2018) 152–161.
[28] M. Tittl, E. Polska, K. Kircher, et al., Topical fundus pulsation measurement in patients with active central serous chorioretinopathy, Arch. Ophthalmol. 121 (7) (2003) 975–978.
[29] N. Imanaga, N. Terao, S. Sawaguchi, et al., Clinical factors related to loculation of fluid in central serous chorioretinopathy, Am. J. Ophthalmol. 235 (2022) 197–203.
[30] R.F. Spaide, C.M. Gemmy Cheung, H. Matsumoto, et al., Venous overload choroidopathy: a hypothetical framework for central serous chorioretinopathy and allied disorders, Prog. Retin. Eye Res. 86 (2022), 100973.

[31] S. Sonoda, T. Sakamoto, T. Yamashita, et al., Luminal and stromal areas of choroid determined by binarization method of optical coherence tomographic images, Am. J. Ophthalmol. 159 (6) (2015) 1123–1131, e1121.
[32] R. Agrawal, X. Wei, A. Goud, K.K. Vupparaboina, S. Jana, J. Chhablani, Influence of scanning area on choroidal vascularity index measurement using optical coherence tomography, Acta Ophthalmol. 95 (8) (2017) e770–e775.
[33] D.L. Nickla, J. Wallman, The multifunctional choroid, Prog. Retin. Eye Res. 29 (2) (2010) 144–168.
[34] T. Murakami, A. Uji, K. Ogino, et al., Association between perifoveal hyperfluorescence and serous retinal detachment in diabetic macular edema, Ophthalmology 120 (12) (2013) 2596–2603.
[35] Y. Muraoka, T. Murakami, K. Nishijima, et al., Association between retinal venular dilation and serous retinal detachment in diabetic macular edema, Retina 34 (4) (2014) 725–731.
[36] K. Shimizu, K. Ujiie, Structure of Ocular Vessels, Igaku-Shoin, 1978.
[37] K.B. Freund, D. Sarraf, B.C.S. Leong, S.T. Garrity, K.K. Vupparaboina, K.K. Dansingani, Association of optical coherence tomography angiography of collaterals in retinal vein occlusion with major venous outflow through the deep vascular complex, JAMA Ophthalmol 136 (11) (2018) 1262–1270.
[38] S.S. Hayreh, M.B. Zimmerman, Branch retinal vein occlusion: natural history of visual outcome, JAMA Ophthalmol 132 (1) (2014) 13–22.